Motion Encoding and Decoding in the Turtle Retina

Mervyn P. B. Ekanayake, Bijoy K. Ghosh, and Philip S. Ulinski

Abstract— **The turtle retina is organized with predominantly two important classes of cells. The first, known as A cells, is sensitive only to light intensity. The other, known as B cells, is also sensitive to direction of targets. We propose models for both types of cells and demonstrate results the models yield. We also show the encoding properties of a single cells and show how a single B-cell can be used in an input discrimination task.**

I. INTRODUCTION

Ever since scientists discovered neurons, they have been trying to understand how they function – especially how they are used in encoding sensory signals and how they communicate to perform control tasks. Although some mathematical descriptions of nerve and muscle membrane properties preceded the monumental work of Hodgkin and Huxley [1], it was their equations for ionic channels that created the natural starting point for the discipline of computational neuroscience. This led to various types of mathematical models of neurons, enabling us to treat them as nonlinear dynamic systems driven by sets of differential equations. Using a suitable model of neurons, a software called GENESIS [11] was developed. GENESIS was found to be especially suitable for large scale models. Our earlier work [12], particularly, had focused primarily on making a large scale model of the visual cortex of freshwater turtles. The goal was to understand how sensory stimuli produce waves of activity in the cortex and what role does these waves play.

This paper describes a model of the turtle retina aiming to understand how signals are processed by the turtle retina. The turtle retina is distinctly different from those of many other animals such as humans and monkeys. The retina contains predominantly two kinds of cells, the A-cells that are sensitive to the light intensity and the B-cells that are sensitive to the direction of motion induced by an optical flow on the retina [5]. These cells are concentrated along a line called the visual streak as opposed to a central point called fovea observed in many other species. Thus a turtle is able to see the motion of moving targets that are projected along the 'streak'. Our goal in this paper is to describe how this motion estimation is carried out at the single cell level.

We study the problem of motion estimation by first making a model of the turtle retinal cells. Retinal cells are subjected to motion inputs with targets of different sizes and moving at different angles with respect to a preferred direction. The firing activities of the cells are noted and their corresponding histograms are computed, and later to apply detection algorithms to perform a detection task.

II. BIO-REALISTIC MODEL OF THE TURTLE RETINAL CELLS

The development of a bio-realistic model for the different types of cells found on the turtle retina was initiated by Ulinski and Baker in 2001. The model is implemented at two levels: the photoreceptor stage, which accepts the visual input and which does the initial processing is developed on MATLAB, and the second stage of ganglion cells, of which, models are developed on GENESIS neuron simulator.

The first stage of the model generates the excitatory and inhibitory conductance response, presynaptic to the second stage of ganglion cells, corresponding to the visual stimulus.

The model accounts for many important natural functions of the retinal ganglion cells, including the different receptor field structures (ON-Center

Mervyn P. B. Ekanayake and Bijoy K. Ghosh are with Department of Mathematics and Statistics, Texas Tech University, Lubbock, TX 79409, USA. mpb.ekanayake@ttu.edu, bijoy.ghosh@ttu.edu

Philip S. Ulinski is with the Department Organismal Biology and Anatomy, University of Chicago, Chicago, IL 60637, USA pulinski@uchicago.edu

and OFF-Center in A-Cells and ON/OFF in B-Cells [6]) sizes, directional sensitivities (in B-Cells) [6], adaptation to light intensity [7], temporal memory, etc. (See Fig. 1.)

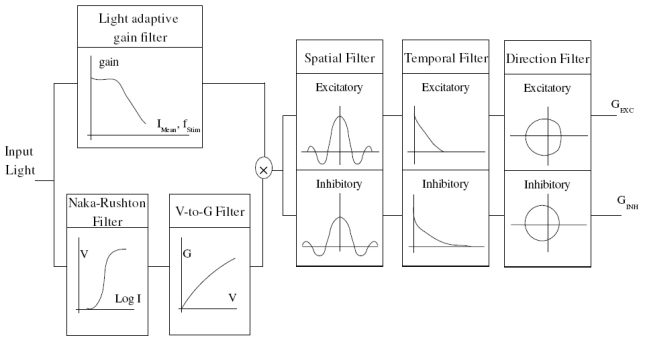

Fig. 1: Functional block diagram of a turtle retinal ganglion cell

1) Basic Conductance Signal: The basic conductance signal is computed at each spatial location. It is generated in two steps. First, the visual (light) signal is passed through a nonlinear saturation filter, called the Naka-Rushton Filter [8].

$$V_R = V_{RM} \frac{I^n}{I^n + a^n}, \tag{1}$$

where, I_n is the input light intensity at each spatial location, V_{RM}, a and n are constants for a cell.

Subsequently, the resulting V_R signal is passed through another filter G to obtain the basic conductance signal [8].

$$G(V_R) = g_{max} + \frac{E_{rest} - V_R - E'_{rest}}{R_{in}\left(E_{rest} - V_R - E_{Na^+}\right)} \tag{2}$$

where, V is the voltage signal created at the previous block, E_{rest}, E'_{rest}, E_{Na^+}, are respectively the resting membrane potential, resting membrane potential with all Na channels closed, and the sodium channel reversal potential, and g_{max} is a constant. The conductance signal generated in this step is later modulated using various filters to condition on the properties of the cells.

2) Spatial Filters: The spatial filters characterize the inherent receptor field structure of the ganglion cells [9]. In terms of implementation, The spacial filter multiplies the conductance signal at each spatial location. The A cells could be one of two kinds. The first, termed A-ON cells, have excitatory center and an inhibitory surrounding. The second type of cell has an inhibitory center and excitatory surrounding. Those are called A-OFF cells. The receptor field structure of A cells are modeled as being the difference of Gaussian functions.

$$G_A(x,y) = k_e e^{-r^2/2\sigma_e^2} - k_i e^{-r^2/2\sigma_i^2}, \tag{3}$$

where $r = \sqrt{x^2 + y^2}$ with (x, y) being the spatial coordinates. The B cells have a slightly more complicated structure. They have an excitatory center, an inhibitory rim and another excitatory rim after that. This structure is modeled as a Gabor function:

$$\begin{aligned} G_B(x,y) &= k e^{-r^2/2\sigma^2}.\cos(2\pi f r) \\ &= k e^{-r^2/2\sigma^2}.\cos^2(\pi f r) \\ &\quad -k e^{-r^2/2\sigma^2}.\sin^2(\pi f r) \end{aligned} \tag{4}$$

In this formulation, the cosine-squared term represents the excitatory regions and the sine-squared term represents the inhibitory region.

3) Directional Filters: The B-cells are sensitive to the direction of the motion (θ) of the visual stimuli [9]. This phenomena is modeled with the directional filter given in 5, which multiplies the basic conductance signal at each spatial location.

$$d(\theta) = a\left(1 + b\cos(\theta - \phi)\right). \tag{5}$$

This filter is only applied to the B cells.

The parameter values a and b are different for the excitatory and the inhibitory parts. Here ϕ is the preferred direction of the cell [5], and 3 principle preferred directions are assumed to be $180°$, $40°$ and $-75°$.

4) The Light Adaptive Filter: The input light is used to compute the gain of the light adaptive gain filter. This is basically a low pass filter calculated at each spatial location and is given in 6. The computed gain will multiply the conductance signal. The filter transfer function is dependent on the mean light intensity, I_0, and it is expressed as a function of frequency of light variation, f, (not the frequency of the light as on the electromagnetic spectrum). The filter has a large gain for low frequencies and low light intensities. Effectively,

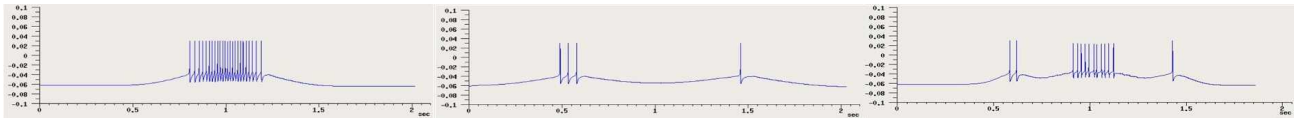

(a) A-on cell response (b) A-off cell response (c) B cell response for preferred direction

Fig. 2: Generated action potentials

it enhances slow varying dim signals, which could otherwise go unrecognized [7]

$$H(f, I_0) = H_n \left(\frac{A(f)}{1 + I_0 B(f)} \right) \tag{6}$$

5) Temporal Filter: The temporal filters models dependence of the past inputs in producing the present output by the retinal ganglions [10]. This is basically a low pass filter so that the temporal convolution is taken between the filter time-response and the conductance signal. Temporal response of the excitatory and inhibitory areas are not the same. Therefore, two temporal time constants are assumed. The temporal response is then modeled as in 7:

$$s(t) = ae^{-t/\tau_a} - be^{-t/\tau_b}. \tag{7}$$

Here a, b, τ_a and τ_b are constants.

Since the light adaptation, spatial, temporal and directional filters are all linear filters, they can be applied in any order. Finally, to generate the synaptic conductance for each cell, the spatial conductance signal is summed up over the receptor field of the cell.

6) Neuron Model: The conductance signals of the first stage generated by MATLAB is provided as the input to the neuron model in the GENESIS neuron simulator as synaptic conductances given by equation 8.

$$I_{input} = G_{ex}(t)(V - E_{ex}) + G_{inh}(t)(V - E_{inh}). \tag{8}$$

E_{ex} and E_{inh} represents the synaptic reversal potentials respectively and modeled with values of 0 mV and -70 mV respectively.

The retinal Ganglion Cell is modeled as a single compartmental model with ionic channels for sodium, potassium and calcium. Further more, channels representing the dynamics of the calcium concentration and after hyperpolarization potassium conductance are also employed. As such, it implements a detailed Hodgkin-Huxley model, accounting for all the essential channels including calcium channel adaptation. Noise was introduced to the ganglion cell model to replicate various uncertainties that are present in nature.

7) Model validation: The model results were compared with [15]. Accordingly, the sensitivity parameters of the models were varied until the spike frequencies were a close match to what is given there.

III. Response of Single Cells Under Different Input Conditions

Multiple simulations were carried out at a single cell level as well as on small collections of retinal cells (retinal patches) subjected to various motion inputs. The stimulus used was a circular spot of light in a dark background. An example of the different sizes and the motion classes studied are shown in Fig. 3. In that figure, the solid lines represent the cell and the excitatory-inhibitory-excitatory regions by the different shadings. The dashed lines represents the size of the spot stimulus used in relation to the cell and its regions.

The responses of the model cells are generated as time varying traces of action potential as shown in Fig. 2. The spike data is extracted from the action potentials traces by thresholding. In this

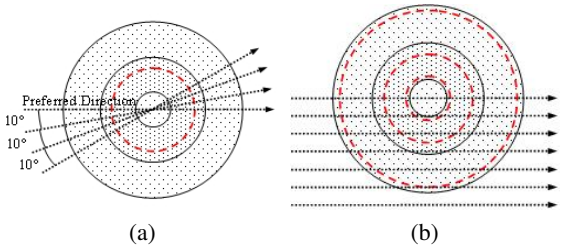

(a) (b)

Fig. 3: (a) Four different angles from the preferred direction (b) Motion of stimulus for the 'shift' experiment

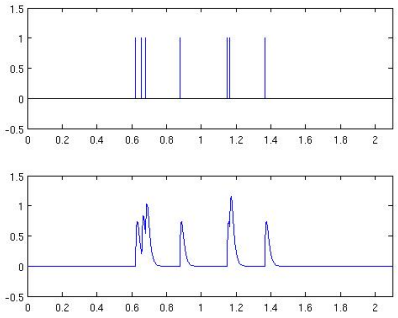

Fig. 4: Low-pass Filtering of the spike train demonstrating the charging and discharging properties of it.

process, if the action potential exceeds a threshold value, it is considered to have made a spike. The spike data is referred to as the spike train.

The relationship between the motion parameters and the cell response can be quantified by various means. One approach employed in this paper is using the peak value of the lowpass filtered spike train, $s(t)$. The other is the L^2 norm (or the root-mean-square value) of the lowpass filtered spike train defined as in 9:

$$||s(t)||_{L^2} = \sqrt{\frac{1}{T}\int_T s^2(t)\,dt}. \tag{9}$$

In order to capture and preserve both spike frequency and timing, spike trains were low-pass filtered using a second order filter with a fast time constant (see Fig. 4).

It was observed that the response of B Cells, when subjected to various stimuli with different orientations and shifts, are best characterized using the peak value of the low pass filtered spike train (see Fig. 5b). The response of A Cells when subjected to stimuli of different shifts were best characterized by using the L^2 norm (see Fig. 5a). The afore mentioned figures were generated in an experiment where the size of the cell, size of the stimulus and the speed of the stimulus was set to pre-determined constant values.

IV. Application to an Input Discrimination Problem

It can be clearly seen from Fig. 5 that the parameters of the stimuli, such as the motion

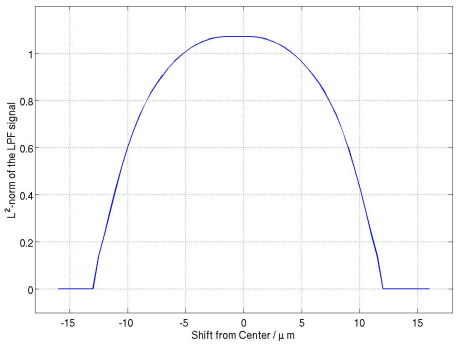

(a) Mean A Cell response

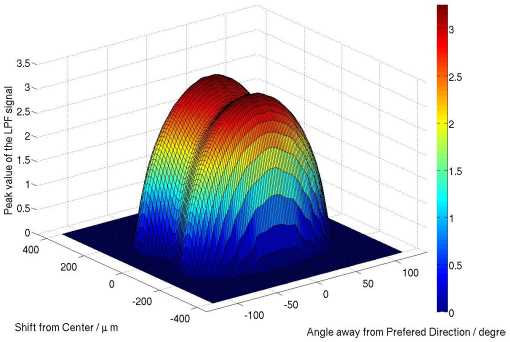

(b) Mean B Cell response

Fig. 5: Mean response of A and B cells for linear motions described in Fig. 3.

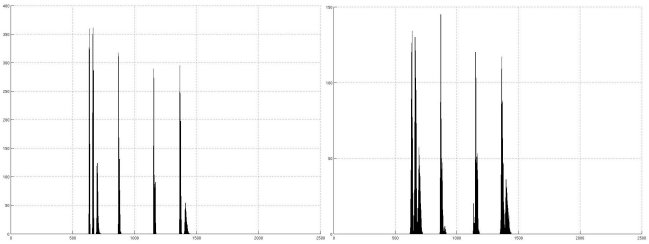

(a) Lower noise (b) Higher noise

Fig. 6: Histogram of spiking activities

direction as well as the distance from the center of the cell to the motion trajectory of the stimuli, affect the response of the ganglion cells of a turtle. In the This section we wish to employ this to a more practical use of discrimination of stimuli moving in different directions. In particular, we try to differentiate between four different directions with respect to the preferred direction of a B Cell.

As a precursor to the input discrimination problem, we looked at the variation of the cell response

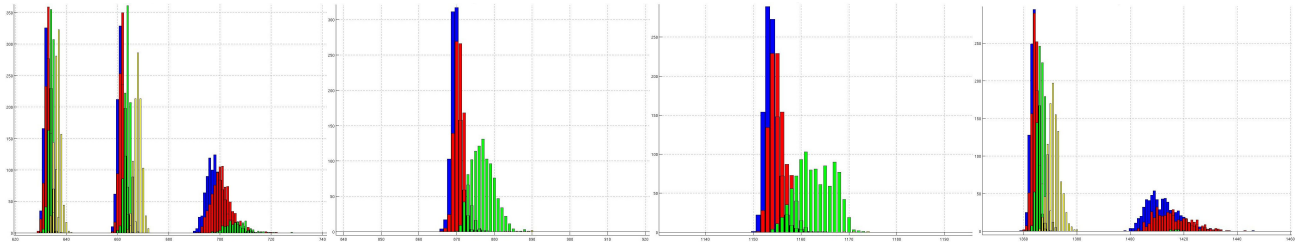

(a) Spike group 1 (b) Spike group 2 (c) Spike group 3 (d) Spike group 4

Fig. 7: Enlarged view of the histogram in Fig. 6 with lower noise. The four colors indicate the four different input angles.

as a distribution. For this purpose, the responses of the cell have been looked at for multiple simulations and a density function is plotted (see Fig. 7) which measures the probability that the cell fires in a given time window. The plots show the pattern as to how the density function changes when stimuli along four different orientations (along the prefered direction, 10° away, 20° away and 30° away from the preferred direction).

Just as when mean response was considered in Fig. 5, it can be seen, from Fig. 7 that there are clear distinctions between the distribution of spikes corresponding to each input condition. This is a clear indication that it should be possible to formulate a detection problem using techniques already established in [13] and [14]. In particular, using a distance metric between any given unknown spike train and each of the spike distributions, and using the method of Principal Component Analysis (K-L decomposition).

Unlike in the case of the turtle visual cortex discussed in [13] and [14], the detection problem using single cells only has a temporal spike sequence. Therefore, one step of K-L decomposition would suffice for this problem. The primary assumption of the detection problem is that, the information content of the spike sequence is captured in both spike frequency as well as spike timing.

Let x_{ij} be the i^{th} low-pass filtered spike train data set, corresponding to the j^{th} input. It consists of t sample points in time (i.e. a $t \times 1$ vector). Suppose, for each of M input conditions ($M = 4$ in this case) the simulation is repeated N times. Then, for each simulation, a $t \times N$ matrix, Γ_j is constructed by augmenting the the time series data into columns. The covariance matrix C_j is calculated for each input condition using $C_j = \Gamma_j \Gamma_j^T$, with $j = 1, \ldots, M$ inputs. The mean covariance matrix C is then computed using equation 10 below:

$$C = \frac{1}{MN} \sum_{j=1}^{M} C_j. \tag{10}$$

The three principal eigenvectors of C are then chosen to be corresponded to the three largest eigenvalues of the C matrices. Once the three principal eigenvectors, $\{\phi_1, \phi_2, \phi_3\}$ are identified, each of the filtered spike trains are projected on to $\{\phi_1, \phi_2, \phi_3\}$ and coordinates $(\alpha_1, \alpha_2, \alpha_3)$ are calculated for each x_{ij} using equation 11 below.

$$\alpha_{k,ij} = \frac{\langle x_{ij}, \phi_k \rangle}{\langle \phi_k, \phi_k \rangle}. \tag{11}$$

Here $i = 1, \ldots, N$, $j = 1, \ldots, M$, $k = 1, 2, 3$ and $\langle \cdot, \cdot \rangle$ denotes the dot product. Each triplet of $(\alpha_{1,ij}, \alpha_{2,ij}, \alpha_{3,ij})$ is then plotted in $\mathbb{R}^3$. This is shown for the low noise case in Fig. 8.

These two figures indicate that each input corresponds to different clusters of principle components. Except when the angles are 0° and 10°, the principle components overlap significantly in $\mathbb{R}^3$. Further more, in contrast to what was seen with the visual cortex in in[13] and [14], we can see that the data points corresponding one input are divided in to a (a small) finite number of sub clusters in the Principal Component Space. The authors conclude that this is due to the difference of number of spikes in each simulation resultant from noise present in the model.

Therefore, we should be able to calculate the probability that a particular point η in the Principal

Component Space is due to the p^{th} input. The complication in this case that, even for the same input, there are several possible clusters to which the result could belong. This adds to the complexity of the detection problem. The detection problem is approached in two steps. First, given a point, it should be estimated to which cluster it belongs. Then, using the cluster it is possible to estimate the input by the methods of maximum likelihood estimation under the hypothesis of Gaussian distribution of points within a given cluster.

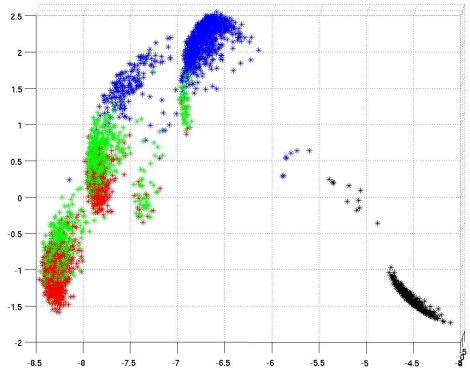

Fig. 8: Principal Components For the low noise case, plotted in $\mathbb{R}^3$. The four colors indicate the four different input angles.

V. Results and Conclusions

This paper provides an outline of the work on building a bio-realistic model of turtle retina. It describes the work in several levels. First, it provides the details of modeling the functionality of a single retinal ganglion cell, and describes how the main types of cells of the retina are modeled. Then it discusses some specific motion encoding properties of the cells. Finally, it discusses how a specific retinal ganglion cell can be used for a motion detection task. This detection problem is different from many other detection problems because there are sub-clusters of data points resulted upon performing Principal Component Analysis. This makes the detection problem a little bit more challenging.

VI. Future Goals

In the future we will continue this study to estimate motion parameters in the optical flow on the retina induced by moving spots with different speeds and directions. This study, which has been initiated for a single B-cell will be extended to a small retinal patch at various locations of the streak. We would also like to study the structural significance of the visual streak especially the relevance of the observed distribution of the A and B cells. Furthermore, we would connect the retina model to the model of the turtle visual cortex, to provide a complete picture of the retino-cortical pathway.

References

[1] Hodgkin, A. L., Huxley, A. F., "A quantitative description of membrane current and its application to conduction and excitation in nerve," J. Physiol., vol. 117, pp. 500–544, 1952.

[2] Peterson, E. H., Ulinski, P. S., "Qunatitative Studies of Retinal Ganglion Cells in a Turtle, Pseudemys scripta elegans: I. Number and Distribution of Ganglion Cells", The Journal of Comparative Neurology, vol. 186, pp. 17–42, 1979.

[3] Peterson, E. H., Ulinski, P. S., "Qunatitative Studies of Retinal Ganglion Cells in a Turtle, Pseudemys scripta elegans: II. Size Spectrum of Ganglion Cells and its Regional Variation", The Journal of Comparative Neurology, vol. 208, pp. 157–168, 1982.

[4] Rodieck, R. D., The First Steps in Seeing, SINAUER, pp. 200–201, 1998.

[5] Bowling, D. B., "Light Responses of ganglion Cells in the Retina of the Turtle", The Journal of Physiology, vol. 299, pp. 173–196, 1980.

[6] Dearworth Jr., J. R., Granda, A. M. "Multiplied Functions unify Shapes of Ganglion-Cell Receptive Fields in Retina of a Turtle", Journal of Vision, vol. 2, pp. 204–217, 2002.

[7] Tranchina, D., Gordon, J., Shapely, R. M., "Retinal Light Adapatiation Evidence for Feedback Mechanism", Nature, vol. 310, pp. 314–316, 1984.

[8] Baylor D. A., Hodgkin A. L., "Detection and Resolution of Visual Stimuli by turtle Photoreceptors", J. Physiol., (Lond.), vol. 234, pp. 163–198, 1973.

[9] Granda A. M., Fulbrook J. E., "Classification of the turtle ganglion cells", J. Neurophysiol., vol. 62, pp. 723–737, 1989.

[10] Borg-Graham L. J., "The computation of directionaly selectivity in the retina occures presenaptic to the ganglion cell" Nature. Neurosci., vol. 4, pp. 176–183, 2001.

[11] Bower, J. M. and Beeman, D., The Book of Genesis, Santa Clara, CA, TELOS, 1998.

[12] Nenadic, Z., Ghosh, B. K. and Ulinski, P., "Modeling and estimation problems in the turtle visual cortex," IEEE Trans. Biomed. Engg., vol. 49. no. 8, pp. 753–762, Aug. 2002.

[13] Du, X., Ghosh, B. K., Ulinski., P. S., "Encoding and Decoding Target Locations with Waves in the Turtle Visual Cortex," IEEE Trans. on Biomedical Engineering, vol. 52, no. 4, pp. 566-577, April 2005.

[14] Du, X., Ghosh, B. K., Ulinski., P. S., "Encoding of Motion Targets by Waves in the Turtle Visual Cortex," IEEE Trans. on Biomedical Engineering, vol. 53, pp. 1688-1695, Aug. 2006.

[15] Marchiafava, P. L., and Weiler, R., "Intracellular analysis and structural correlates of the organization of inputs to ganglion cells in the retina of the turtle" Proc. R. Soc. Lond., vol. 208, pp. 103-113, 1980.